This is a previous version of the article published in International Journal of Systems Science. 2024, 55(5): 954-979. https://doi.org/10.1080/00207721.2023.2301040

# Flatness-based control in successive loops for robotic manipulators and autonomous vehicles

G. Rigatos[a] M. Abbaszadeh[b] J. Pomares[c] G. Cuccurullo[d]

[a]Unit Industrial Autom.
Industrial Systems Inst.
26504, Patras, Greece
grigat@ieee.org

[b]Dept. ECS Eng.
Rensselaer Polytech. Inst.
12065, NY, USA
masouda@ualberta.ca

[c]Dept. of Systems Eng
Univ. of Alicante
03690, Alicante, Spain
jpomares@gcloud.ua.es

[d]Dept. of Industrial Eng.
Univ. of Salerno
84084, Fisciano, Italy
gcuccurullo@unisa.it

**Abstract**: The control problem for the multivariable and nonlinear dynamics of robotic manipulators and autonomous vehicles is solved with the use of a flatness-based control approach which is implemented in successive loops. The state-space model of these robotic systems is separated into two subsystems, which are connected between them in cascading loops. Each one of these subsystems can be viewed independently as a differentially flat system and control about it can be performed with inversion of its dynamics as in the case of input-output linearized flat systems. The state variables of the second subsystem become virtual control inputs for the first subsystem. In turn exogenous control inputs are applied to the first subsystem. The whole control method is implemented in two successive loops and its global stability properties are also proven through Lyapunov stability analysis. The validity of the control method is confirmed in two case studies: (a) control of a 3-DOF industrial rigid-link robotic manipulator, (ii) control of a 3-DOF autonomous underwater vessel.

**Keywords**: robotic manipulators, autonomous underwater vessels, multivariable control, differential flatness properties, flatness-based control in successive loops, global stability, Lyapunov analysis.

## 1 Introduction

Differential flatness theory is currently a main direction in nonlinear control systems analysis and synthesis [1-6]. A system is considered to be differentially flat if all its state variables and its control inputs can be expressed as functions of one single algebraic variable which is the so-called flat output, and also as functions of the flat-output's derivatives [7-10]. The differential flatness property enables the transformation of the nonlinear system's dynamics in the linear canonical form [11-15]. The latter description is controllable and observable thus allowing to treat effectively control and estimation problems [16-19]. In this paper, a successive loops approach is developed for controller design in nonlinear dynamical systems which exhibit the differential flatness property. The method makes use of the initial nonlinear model of the system and of its decomposition into a set of nonlinear subsystems for which the differential flatness property holds [20-24].

The proposed control method is directly applicable to nonlinear systems of the so-called triangular form, or to system's which can be transformed into such a form [1],[2]. The state-space model of the nonlinear system is decomposed into subsystems, which satisfy differential flatness properties. For each subsystem of the state-space model a virtual control input is computed, capable of inverting the subsystem's dynamics and of eliminating the subsystem's tracking error. The control input that is actually applied to the nonlinear system is found from the last row of the state-space description. This control input incorporates in a recursive manner all virtual control inputs which were computed for the individual subsystems associated with the initial state-space equation. The control input that should be applied to the nonlinear system so as to assure that all its state vector elements will converge to the desirable setpoints, is obtained at each iteration of the control algorithm, by tracing the subsystems of the state-space model backwards.

The proposed method of flatness-based control in successive loops is applied to the control problem of the multivariable and nonlinear dynamics of robotic manipulators and autonomous vehicles [1],[2]. The state-space model of these robotic systems is separated into two subsystems, which are connected between them in cascading loops. Each one of these subsystems can be viewed independently as a differentially flat system and control about it can be performed with inversion of its dynamics as in the case of input-output linearized flat systems. The state variables of the second subsystem become virtual control inputs for the first subsystem. In turn exogenous control inputs are applied to the first subsystem. The whole control method is implemented in two successive loops and its global stability properties are also proven through Lyapunov stability analysis. The following application examples have confirmed the method's fine performance: (a) control of a 3-DOF industrial rigid-link robotic manipulator, (ii) control of a 3-DOF autonomous underwater vessel.

The structure of the paper is as follows: in Section 2 the concept of flatness-based control in successive loops and its use in nonlinear dynamical systems is analyzed. The method's stability properties are analyzed. In Section 3 the flatness-based control method is successive loops is applied to the model of the 3-DOF redundant planar robotic manipulator. In Section 4 the flatness-based control method in successive loops is applied to the model of the 3-DOF autonomous underwater vessel. In Section 5 the performance of the control method when used in the above noted nonlinear robotic systems is evaluated through simulation experiments. Finally, in Section 6 concluding remarks are stated. Moreover, in an Appendix which appears in the end of the manuscript a comparison between flatness-based control in successive loops and backstepping control is provided.

## 2 Flatness-based control in successive loops for nonlinear dynamical systems

### 2.1 Decomposition of the state-space model into cascading differentially flat subsystems

The following nonlinear dynamical system is now examined:

$$\begin{matrix} \dot{x} = f(x) + g(x)u \ x{\in}R^m \quad u{\in}R^q \\ y = h(x) \end{matrix} \tag{1}$$

Moreover, it is considered that the system can be decomposed into $n$ subsystems which have the so-called triangular form :

$$\begin{matrix} \dot{x}_1 = f_1(x_1) + g_1(x_1)x_2 \\ \dot{x}_2 = f_2(x_1,x_2) + g_2(x_1,x_2)x_3 \\ \dot{x}_3 = f_3(x_1,x_2,x_3) + g_3(x_1,x_2,x_3)x_4 \\ \cdots \\ \dot{x}_i = f_i(x_1,x_2,\cdots,x_i) + g_i(x_1,x_2,\cdots,x_i)x_{i+1} \\ \cdots \\ \dot{x}_{n-1} = f_{n-1}(x_1,x_2,\cdots,x_{n-1}) + g_{n-1}(x_1,x_2,\cdots,x_{n-1})x_n \\ \dot{x}_n = f_n(x_1,x_2,\cdots,x_n) + g_n(x_1,x_2,\cdots,x_n)u \end{matrix} \tag{2}$$

The following virtual control inputs $\alpha_i = x_{i+1}$ are defined for the $i$=th subsystem of the state-space model of Eq. (2)

$$
\begin{aligned}
\dot{x}_1 &= f_1(x_1) + g_1(x_1)\alpha_1 \\
\dot{x}_2 &= f_2(x_1,x_2) + g_2(x_1,x_2)\alpha_2 \\
\dot{x}_3 &= f_3(x_1,x_2,x_3) + g_3(x_1,x_2,x_3)\alpha_3 \\
&\cdots \\
\dot{x}_i &= f_i(x_1,x_2,\cdots,x_i) + g_i(x_1,x_2,\cdots,x_i)\alpha_i \\
&\cdots \\
\dot{x}_{n-1} &= f_{n-1}(x_1,x_2,\cdots,x_{n-1}) + g_{n-1}(x_1,x_2,\cdots,x_{n-1})\alpha_{n-1} \\
\dot{x}_n &= f_n(x_1,x_2,\cdots,x_n) + g_n(x_1,x_2,\cdots,x_n)u
\end{aligned}
\tag{3}
$$

The system of Eq. (3) is a differentially flat one. It is considered that $y = x_1$ is the flat output of system. It can be easily shown that each virtual control input $\alpha_i = x_{i+1}$, $i = 1, 2, \cdots$ can be expressed as a function of the flat output and its derivatives, since it holds

$$\alpha_i = \frac{1}{g_i(x_1,x_2,\cdots,x_i)}(\dot{x}_i - f_(x_1,x_2,\cdots,x_i)) \tag{4}$$

For $i = 1$ one has

$$\alpha_1 = \frac{1}{g_1(x_1}(\dot{x}_1 - f_(x_1) \tag{5}$$

which means that $\alpha_1$ is a function of the flat output and its derivative. For $i = 2$ one has

$$\alpha_2 = \frac{1}{g_2(x_1,x_2)}(\dot{x}_2 - f_2(x_1,x_2) \tag{6}$$

which means that $\alpha_2 = x_3$ is a function of the flat output $y = x_1$ and its derivatives. Continuing in a similar manner one has that $\alpha_{n-1} = x_n$ and consequently $\alpha_n = u$ is also a function of the flat output $y = x_1$ and its derivatives. According to the above, one has a nonlinear dynamical system in which, all its state variables and the control input can be written as functions of the flat output and its derivatives. Therefore, such a system is differentially flat.

Additionally, by considering each subsystem of the model of Eq. (3), one has a set of $n$ subsystems of the form

$$\dot{x}_i = f_i(x_1,x_2,\cdots,x_i) + g_i(x_1,x_2,\cdots,x_i)\alpha_i \tag{7}$$

where each subsystem describes the dynamics of the single state variable $x_i$. For each one of these subsystems one can consider the state variable $x_i$ as the flat output. Obviously, the virtual control input $\alpha_i$ is a function of this flat output and its derivatives. Therefore, each local subsystem is also differentially flat.

Next, one can compute the virtual inputs which are applied to each subsystem. For the first subsystem, which is associated with the first row of Eq. (2), and by defining $z_i = x_i - x_i^* = x_1 - \alpha_{i-1}$, the virtual control input is given by

$$
\begin{aligned}
\alpha_1 = x_2^* &= \frac{1}{g_1(x_1)}(\dot{x}_1^* - f_(x_1) - K_1^1(x_1 - x_1^*)) \Rightarrow \\
\alpha_1 = x_2^* &= \frac{1}{g_1(x_1)}(\dot{x}_1^* - f_(x_1) - K_1^1 z_1)
\end{aligned}
\tag{8}
$$

From the second row of Eq. (2), and using that $z_2 = x_2 - x_2^* = x_2 - \alpha_1$ one has

$$
\begin{aligned}
\alpha_2 = x_3^* &= \frac{1}{g_2(x_1,x_2)}(\dot{x}_2^* - f_2(x_1,x_2) - K_1^2(x_2 - x_2^*)) \Rightarrow \\
\alpha_2 = x_3^* &= \frac{1}{g_2(x_1,x_2)}(\dot{\alpha}_1 - f_2(x_1,x_2) - K_1^2 z_2)
\end{aligned}
\tag{9}
$$

From the third row of Eq. (2), and using that $z_3 = x_3 - x_3^* = x_3 - \alpha_2$ one has

$$\alpha_3 = x_4^* = \frac{1}{g_3(x_1,x_2,x_3)}(\dot{x}_3^* - f_3(x_1,x_2,x_3) - K_1^3(x_3 - x_3^*)) \Rightarrow$$
$$\alpha_3 = x_4^* = \frac{1}{g_3(x_1,x_2,x_3)}(\dot{\alpha}_2 - f_3(x_1,x_2,x_3) - K_1^3 z_3) \tag{10}$$

Continuing in a similar manner and from the $i$-th row of the state-space description of the system given in Eq. (2), and while also using that $z_i = x_i - x_i^* = x_i - \alpha_{i-1}$ one obtains

$$\alpha_i = x_{i+1}^* = \frac{1}{g_i(x_1,x_2,\cdots,x_i)}(\dot{x}_i^* - f_i(x_1,x_2,\cdots,x_i) - K_1^i(x_i - x_i^*)) \Rightarrow$$
$$\alpha_i = x_{i+1}^* = \frac{1}{g_i(x_1,x_2,\cdots,x_i)}(\dot{\alpha}_{i-1} - f_i(x_1,x_2,\cdots,x_3) - K_1^i z_i) \tag{11}$$

Equivalently, from the $n-1$-th row of the state-space model of Eq. (2) and using that $z_{n-1} = x_{n-1} - x_{n-1}^* = x_{n-1} - \alpha_{n-2}$ one has

$$\alpha_{n-1} = x_n^* = \frac{1}{g_{n-1}(x_1,x_2,\cdots,x_{n-1})}(\dot{x}_{n-1}^* - f_{n-1}(x_1,x_2,\cdots,x_{n-1}) - K_1^{n-1}(x_{n-1} - x_{n-1}^*)) \Rightarrow$$
$$\alpha_{n-1} = x_n^* = \frac{1}{g_{n-1}(x_1,x_2,\cdots,x_{n-1})}(\dot{\alpha}_{n-2} - f_{n-1}(x_1,x_2,\cdots,x_{n-1}) - K_1^{n-1} z_{n-1}) \tag{12}$$

Finally, from the $n$-th row of the state-space model of Eq. (2) and using that $z_n = x_n - x_n^* = x_n - \alpha_{n-1}$ one has

$$\alpha_n = u = \frac{1}{g_n(x_1,x_2,\cdots,x_n)}(\dot{x}_n^* - f_n(x_1,x_2,\cdots,x_n) - K_1^n(x_n - x_n^*)) \Rightarrow$$
$$\alpha_n = u = \frac{1}{g_n(x_1,x_2,\cdots,x_n)}(\dot{\alpha}_{n-1} - f_n(x_1,x_2,\cdots,x_n) - K_1^n z_n) \tag{13}$$

The computation of the control input $u$ that should be actually applied to the nonlinear system is performed in a recursive manner by processing backwards the virtual control inputs described in Eq. (8) to Eq. (13).

Thus, from the last subsystem of the state-space description the control input that is actually applied to the nonlinear system is found. This control input contains recursively all virtual control inputs which were computed for the individual subsystems associated with the state-space equation. Thus, by tracing the rows of the state-space model backwards, at each iteration of the control algorithm, one can finally obtain the control input that should be applied to the nonlinear system so as to assure that all its state vector elements will converge to the desirable setpoints.

## 2.2 Tracking error dynamics for flatness-based control in successive loops

By substituting Eq. (13) into the last row of the state space model of Eq. (2), and using the definition $x_n - a_{n-1} = z_n$, one obtains:

$$\begin{array}{c} \dot{x}_n = \dot{a}_{n-1} - K_1^n(x_n - \alpha_{n-1}) \Rightarrow \\ (\dot{x}_n - \dot{a}_{n-1}) + K_1^n(x_n - \alpha_{n-1}) = 0 \Rightarrow \\ \dot{z}_n + K_1^n z_n = 0 \end{array} \tag{14}$$

By substituting Eq. (12) into the last row of the state space model of Eq. (2), and using the definition $x_{n-1} - a_{n-2} = z_{n-1}$, one obtains:

$$\begin{gathered}\dot{x}_{n-1}=\dot{a}_{n-2}-K_1^{n-1}(x_{n-1}-\alpha_{n-2})\Rightarrow \\ (\dot{x}_{n-1}-\dot{a}_{n-2})+K_1^{n-1}(x_{n-1}-\alpha_{n-2})=0\Rightarrow \\ \dot{z}_{n-1}+K_1^{n-1}z_{n-1}=0\end{gathered} \tag{15}$$

By substituting Eq. (11) into the last row of the state space model of Eq. (2), and using the definition $x_i-a_{i-1}=z_i$, one obtains:

$$\begin{gathered}\dot{x}_i=\dot{a}_{i-1}-K_1^{n-1}(x_i-\alpha_{i-1})\Rightarrow \\ (\dot{x}_i-\dot{a}_{i-1})+K_1^i(x_i-\alpha_{i-1})=0\Rightarrow \\ \dot{z}_i+K_1^iz_i=0\end{gathered} \tag{16}$$

while continuing backwards and by substituting Eq. (9) into the second row of the state space model of Eq. (2), and using the definition $x_2-a_1=z_2$, one gets:

$$\begin{gathered}\dot{x}_2=\dot{a}_1-K_1^2(x_2-\alpha_1)\Rightarrow \\ (\dot{x}_2-\dot{a}_1)+K_1^2(x_2-\alpha_1)=0\Rightarrow \\ \dot{z}_2+K_1^2z_2=0\end{gathered} \tag{17}$$

Finally, by substituting Eq. (8) into the first row of the state space model of Eq. (2), one has:

$$\begin{gathered}\dot{x}_1=\dot{x}_1-K_1^1(x_1-x_1^d)\Rightarrow \\ (\dot{x}_1-\dot{x}_1^d)+K_1^1(x_1-x_1^d)=0\Rightarrow \\ \dot{z}_1+K_1^1z_1=0\end{gathered} \tag{18}$$

Therefore, after the application of the feedback control law, the closed-loop dynamics becomes $\dot{z}_1+K_1^1z_1=0$, $\dot{z}_2+K_1^2z_2=0$, $\dot{z}_3+K_1^3z_3=0$, $\cdots$, $\dot{z}_i+K_1^iz_i=0$, $\cdots$, $\dot{z}_{n-1}+K_1^{n-1}z_{n-1}=0$, $\dot{z}_n+K_1^nz_n=0$.

In matrix form, the closed-loop dynamics is written as

$$\begin{pmatrix}\dot{z}_1\\ \dot{z}_2\\ \dot{z}_3\\ \cdots\\ \dot{z}_i\\ \cdots\\ \dot{z}_{n-1}\\ \dot{z}_n\end{pmatrix}=\begin{pmatrix}-K_1^1\;0\;0\;\cdots\;0\;\cdots\;0\;0\\ 0\;-K_1^2\;0\;\cdots\;0\;\cdots\;0\;0\\ 0\;0\;-K_1^3\;\cdots\;0\;\cdots\;0\;0\\ \cdots\;\cdots\;\cdots\;\cdots\;\cdots\\ 0\;0\;0\;\cdots\;-K_1^i\;\cdots\;0\;0\\ \cdots\;\cdots\;\cdots\;\cdots\;\cdots\\ 0\;0\;0\;\cdots 0\cdots\;-K_1^{n-1}\;0\\ 0\;0\;0\;\cdots\;0\;\cdots\;0\;-K_1^n\end{pmatrix}\begin{pmatrix}z_1\\ z_2\\ z_3\\ \cdots\\ z_i\\ \cdots\\ z_{n-1}\\ z_n\end{pmatrix} \tag{19}$$

or equivalently

$$\dot{Z}=KZ \tag{20}$$

By selecting the eigenvalues of matrix $K$ to be in the left complex semiplane, one has that

$$lim_{t\to\infty}Z=0_{n\times1} \tag{21}$$

which also implies that $lim_{t\to\infty}x_1=x_1^d$, $lim_{t\to\infty}x_2=\alpha_1=x_2^d$, $lim_{t\to\infty}x_3=\alpha_2=x_3^d$, $\cdots$, $lim_{t\to\infty}x_i=\alpha_{i-1}=x_i^d$, $\cdots$, $lim_{t\to\infty}x_{n-1}=\alpha_{n-2}=x_{n-1}^d$, and $lim_{t\to\infty}x_n=\alpha_{n-1}=x_n^d$.

To prove asymptotic stability for the proposed control scheme the following Lyapunov function can be defined

$$V=\sum_{i=1}^N\frac{1}{2}z_i^2 \tag{22}$$

The time derivative of the aforementioned Lyapunov function is

$$\dot{V} = \sum_{i=1}^{N} z_i \dot{z}_i \Rightarrow \dot{V} = -\sum_{i=1}^{N} K_1^i z_i^2 \Rightarrow \dot{V} < 0 \quad (23)$$

By selecting the feedback control gains $K_1^i,\ i = 1, \cdots, n$ to be $K_1^i > 0$, the asymptotic stability of the control loop is assured.

# 3 Flatness-based control in successive loops for 3-DOF robotic manipulators

## 3.1 Dynamic model of the 3-DOF redundant robotic manipulators

The first test-case for the flatness-based control method in successive loops is concerned with redundant planar robotic manipulators. Control of robotic manipulators with an end-effector that moves in a tasks space with lower dimension than the robot's degrees of freedom comes against the problem of redundancy [25],[26]. Kinematic redundancy occurs when a manipulator has more degrees of freedom than the minimum number required to execute a task. When a manipulator is redundant, it is anticipated that the inverse kinematic problem admits multiple solutions. This means that for a constant position of the end-effector, several configurations of the arm's joints can be obtained [27-28]. Redundant robots achieve a versatile motion in the joints space and dexterity in tasks execution [29]. They can find use in robotic surgery as well as on several industrial tasks, because of offering multiple joints configurations that allow the end effector to reach easier the targeted position in the tasks' space [30].

Generally, redundancy specifies a robot's internal movement without affecting the trajectory of the robot's end effector and permits the robot to react in a better way to the environment that surrounds. This in turn signifies that the robot can achieve obstacles' avoidance and can keep moderate the torques developed by its actuators [31-33]. Control of redundant manipulators, which is also known as redundancy resolution, is to find a control action in the joints' space of a redundant robotic arm that leads to a desired motion of the end-effector in the tasks' space [34-36]. Several approaches have been proposed for the control of redundant robots [38]. The primary objective is to achieve stability properties for the redundant manipulator A related objective is the avoidance of singularities in the robot's inverse kinematic problem [40]. So far the nonlinear optimal control problem for redundant manipulators has been little studied.

The diagram of the 3-DOF redundant planar robotic manipulator is given in Fig. 1 The dynamic model of the 3-DOF redundant robotic manipulator is given by [3]

$$M(\theta)\ddot{\theta} + C(\theta, \dot{\theta}) + G(\theta) = \tau \quad (24)$$

where the robot's inertia matrix is given by

$$M(\theta) = \begin{pmatrix} m_{11} & m_{12} & m_{13} \\ m_{21} & m_{22} & m_{23} \\ m_{31} & m_{32} & m_{33} \end{pmatrix} \quad (25)$$

with $m_{11} = 1_1 + a_2 + a_4 + 2a_3cos(\theta_3) + 2a_5cos(\theta_2 + \theta_3) + 2a_6cos(\theta_3)$, $m_{12} = m_{21} = a_2 + a_4cos(\theta_2) + a_5cos(\theta_2 + \theta_3) + 2a_6cos(\theta_3)$, $m_{13} = m_{31} = a_4 + a_5cos(\theta_2 + \theta_3) + 2a_6cos(\theta_3)$, $m_{22} = a_2 + a_4 + a_6cos(\theta_3)$, $m_{23} = m_{32} = a_4 + a_6cos(\theta_3)$, $m_{33} = a_4$.

where $a_1 = m_1 l_1^2 + I_1 + (m_1 + m_2) l_1^2$, $a_2 = I_2 + m_2 l_2^2$, $a_3 = (m_2 l_2 + m_3 L_2) L_1$, $a_4 = I_3 + m_3 l_3^2$, $a_5 = m_3 l_3 L_1$, $a_6 = m_3 L_2 l_3$.

with $m_i,\ i = 1, 2, 3$ to be the masses of the links, $I_i,\ i = 1, 2, 3$ to be the moments of inertia of the links, $L_, i = 1, 2, 3$ to be the lengths of the links, and $l_i,\ i = 1, 2, 3$ to be the distances between the centers of the

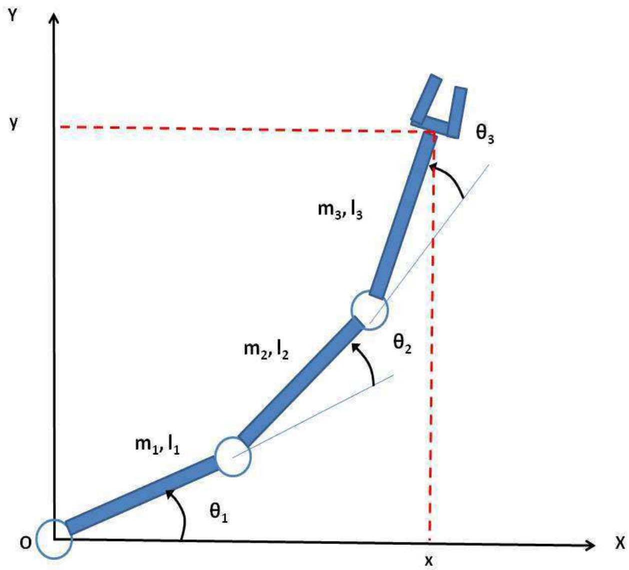


Figure 1: Diagram of the 3-DOF redundant planar robotic manipulator

links and their centers of gravity.

About the Coriolis and centrifugal forces matrix one has

$$C(\theta,\dot{\theta}) = \begin{pmatrix} -a_3(2\dot{\theta}_1+\dot{\theta}_2)\dot{\theta}_2 sin(\theta)_2 \\ -a_5(2\dot{\theta}_1+\dot{\theta}_2+\dot{\theta}_3)(\dot{\theta}_2+\dot{\theta}_3)sin(\theta_2+\theta_3) \\ -a_6(2\dot{\theta}_1+2\dot{\theta}_2+\dot{\theta}_3)\dot{\theta}_3 sin(\theta)_3 \\ \\ -a_3\dot{\theta}_1^2 sin(\theta_2)+a_5\dot{\theta}_1^2 sin(\theta_2+\theta_3)- \\ -a_6(2\dot{\theta}_1+2\dot{\theta}_2+\dot{\theta}_3)\dot{\theta}_3 sin(\theta)_3 \\ \\ a_5\dot{\theta}_1^2 sin(\theta_2+\theta_3)+a_6(\dot{\theta}_1+\dot{\theta}_2)^2 sin(\theta_3) \end{pmatrix} \tag{26}$$

The gravitational forces matrix is taken to have zero elements because the manipulator is planar

$$G(\theta) = \begin{pmatrix} 0 \\ 0 \\ 0 \end{pmatrix} \tag{27}$$

Considering next the sub-determinants of the inertia matrix $M$, the inverse matrix of $M$ is given by

$$M^{-1}(\theta) = \frac{1}{detM}\begin{pmatrix} M_{11} & -M_{21} & M_{31} \\ -M_{12} & M_{22} & -M_{32} \\ M_{13} & -M_{23} & M_{33} \end{pmatrix} \tag{28}$$

Thus, about the dynamic model of the redundant robotic manipulator one has:

$$\begin{pmatrix}\ddot{\theta}_1\\ \ddot{\theta}_2\\ \ddot{\theta}_3\end{pmatrix} = \frac{1}{detM}\begin{pmatrix}M_{11} & -M_{21} & M_{31}\\ -M_{12} & M_{22} & -M_{32}\\ M_{13} & -M_{23} & M_{33}\end{pmatrix}\left[\begin{pmatrix}C_1\\ c_2\\ C_5\end{pmatrix} + \begin{pmatrix}G_1\\ G_2\\ G_3\end{pmatrix}\right] + \frac{1}{detM}\begin{pmatrix}M_{11} & -M_{21} & M_{31}\\ -M_{12} & M_{22} & -M_{32}\\ M_{13} & -M_{23} & M_{33}\end{pmatrix}\begin{pmatrix}\tau_1\\ \tau_2\\ \tau_3\end{pmatrix} \tag{29}$$

After intermediate operations, the dynamic model of the redundant robotic manipulator is written as

$$\begin{pmatrix}\ddot{\theta}_1\\ \ddot{\theta}_2\\ \ddot{\theta}_3\end{pmatrix} = \begin{pmatrix}\frac{-M_{11}(C_1+G_1)+M_{21}(C_2+G_2)-M_{31}(C_3+G_3)}{detM}\\ \frac{M_{12}(C_1+G_1)-M_{22}(C_2+G_2)+M_{32}(C_3+G_3)}{detM}\\ \frac{-M_{13}(C_1+G_1)+M_{23}(C_2+G_2)-M_{33}(C_3+G_3)}{detM}\end{pmatrix} + \begin{pmatrix}\frac{M_{11}}{detM} & -\frac{M_{21}}{detM} & \frac{M_{31}}{detM}\\ -\frac{M_{12}}{detM} & \frac{M_{22}}{detM} & -\frac{M_{32}}{detM}\\ \frac{M_{13}}{detM} & -\frac{M_{23}}{detM} & \frac{M_{33}}{detM}\end{pmatrix}\begin{pmatrix}\tau_1\\ \tau_2\\ \tau_3\end{pmatrix} \tag{30}$$

Next, by defining the state vector $x = [x_1, x_2, x_3, x_4, x_5, x_6]^T = [\theta_1, \theta_2, \theta_3, \dot{\theta}_1, \dot{\theta}_2, \dot{\theta}_3]^T$ one obtains the following state-space description

$$\begin{aligned}
\dot{x}_1 &= x_4\\
\dot{x}_2 &= x_5\\
\dot{x}_3 &= x_6\\
\dot{x}_4 &= \frac{-M_{11}(C_1+G_1)+M_{21}(C_2+G_2)-M_{31}(C_3+G_3)}{detM} + \frac{M_{11}}{detM}\tau_1 - \frac{M_{21}}{setM}\tau_2 + \frac{M_{31}}{detM}\tau_3\\
\dot{x}_5 &= \frac{M_{12}(C_1+G_1)-M_{22}(C_2+G_2)+M_{33}(C_3+G_3)}{detM} - \frac{M_{12}}{detM}\tau_1 + \frac{M_{22}}{detM}\tau_2 - \frac{M_{32}}{detM}\tau_3\\
\dot{x}_6 &= \frac{-M_{13}(C_1+G_1)+M_{23}(C_2+G_2)-M_{33}(C_3+G_3)}{detM} + \frac{M_{13}}{detM}\tau_1 - \frac{M_{23}}{setM}\tau_2 + \frac{M_{33}}{detM}\tau_3
\end{aligned} \tag{31}$$

Equivalently, one has the following state-space description in matrix form

$$\begin{pmatrix}\dot{x}_1\\ \dot{x}_2\\ \dot{x}_3\\ \dot{x}_4\\ \dot{x}_5\\ \dot{x}_6\end{pmatrix} = \begin{pmatrix}x_2\\ x_4\\ x_6\\ \frac{-M_{11}(C_1+G_1)+M_{21}(C_2+G_2)-M_{31}(C_3+G_3)}{detM}\\ \frac{M_{12}(C_1+G_1)-M_{22}(C_2+G_2)+M_{33}(C_3+G_3)}{detM}\\ \frac{-M_{13}(C_1+G_1)+M_{23}(C_2+G_2)-M_{33}(C_3+G_3)}{detM}\end{pmatrix} + \begin{pmatrix}0 & 0 & 0\\ 0 & 0 & 0\\ 0 & 0 & 0\\ \frac{M_{11}}{detM} & -\frac{M_{21}}{setM} & \frac{M_{31}}{detM}\\ -\frac{M_{12}}{detM} & \frac{M_{22}}{detM} & -\frac{M_{32}}{detM}\\ \frac{M_{13}}{detM} & -\frac{M_{23}}{setM} & \frac{M_{33}}{detM}\end{pmatrix}\begin{pmatrix}u_1\\ u_2\\ u_3\end{pmatrix} \tag{32}$$

and equivalently one has the state-space description

$$\begin{pmatrix}\dot{x}_1\\ \dot{x}_2\\ \dot{x}_3\\ \dot{x}_4\\ \dot{x}_5\\ \dot{x}_6\end{pmatrix} = \begin{pmatrix}x_2\\ x_4\\ x_6\\ f_4(x)\\ f_6(x)\\ f_6(x)\end{pmatrix} + \begin{pmatrix}0 & 0 & 0\\ 0 & 0 & 0\\ 0 & 0 & 0\\ g_{41}(x) & g_{42}(x) & g_{43}(x)\\ g_{51}(x) & g_{52}(x) & g_{53}(x)\\ g_{61}(x) & g_{62}(x) & g_{63}(x)\end{pmatrix}\begin{pmatrix}u_1\\ u_2\\ u_3\end{pmatrix} \tag{33}$$

Next, by denoting the state vectors $x_{13} = [x_1, x_2, x_3]^T$, $x_{46} = [x_4, x_5, x_6]^T$, as well as the vectors $f_{33} = [x_4, x_5, x_6]^T$ , $f_{46} = [f_4(x), f_5(x), f_6(x)]^T$ and the matrices $g_{13} = 0_{3\times3}$

$$g_{46} = \begin{pmatrix} g_{41}(x) & g_{42}(x) & g_{43}(x) \\ g_{51}(x) & g_{52}(x) & g_{53}(x) \\ g_{61}(x) & g_{62}(x) & g_{63}(x) \end{pmatrix} \tag{34}$$

the state-space description of the system comes into the following concise (and also triangular) form

$$\begin{pmatrix} \dot{x}_{13} \\ \dot{x}_{46} \end{pmatrix} = \begin{pmatrix} x_{46} \\ f_{46}(x) \end{pmatrix} = \begin{pmatrix} x_{46} \\ f_{46}(x) \end{pmatrix} + \begin{pmatrix} 0_{3\times3} \\ g_{46}(x_{46}) \end{pmatrix} u \tag{35}$$

Equivalently, one has that the dynamics of the redundant robotic manipulator consists of two sub-systems

$$\dot{x}_{13} = x_{46} \tag{36}$$

$$\dot{x}_{46} = f_{46}(x) + g_{46}(x)u \tag{37}$$

It can be proven that the redundant robotic manipulator is a differentially flat system with flat output $y = x_{13}$. Indeed, from Eq. (36) it holds that

$$x_{46} = \dot{x}_{13} \Rightarrow x_{46} = \dot{y} \tag{38}$$

Thus $x_{46}$ is a differential function of the flat output $y = x_{13}$. Moreover, from Eq. (37), and using that $f_{46}(x)$ and $g_{46}(x)$, are functions of $x_{31}$, $x_{46}$ that is of $y$, $\dot{y}$ one has

$$u = g_{46}(x)^{-1}[\dot{x}_{46} - f_{46}(x)] \Rightarrow u = g_{46}(y, \dot{y})^{-1}[\ddot{y} - f_{46}(y, \dot{y})] \tag{39}$$

Consequently, the control input $u$ is also a differential function of the flat output $y = x_{13}$. As a result of the above, the redundant robotic manipulator which consists of the subsystems of Eq. (36) and Eq. (37) is a differentially flat system. As a result of the above, the 3-DOF redundant robotic manipulator manipulator is a differentially flat system.

### 3.2 Flatness-based controller in successive loops for redundant robotic manipulators

One can also demonstrated that the previously noted subsystems of Eq. (36) and Eq. (37) stand independently for differentially flat systems.

For the subsystem of Eq. (36) $x_{13}$ is the flat output and $x_{46}$ is a virtual control input. As shown before, $x_{46}$ is a differential function of the flat output $x_{13}$ and thus the subsystem of Eq. (36) is differentially flat.

For the subsystem of Eq. (37) $x_{46}$ is the flat output. Besides, the state vectors elements of $x_{13}$ are viewed as coefficients and thus functions $f_{46}(x)$ and $g_{46}(x)$ depend only on the flat output $x_{46}$. Furthermore, using again Eq. (39) one has also that the control input $u$ is also a differential function of the flat output $x_{46}$. Consequently, the subsystem of Eq. (37) is also differentially flat.

The control of the subsystems of Eq. (36) and Eq. (37) can be carried out following the design process of controllers for input-output linearized differentially flat systems.

For the subsystem of Eq. (36), the setpoint is denoted as $x_{13}^d$ and the value of the virtual control input $x_{46}$ which stabilizes the system's dynamics is

$$x_{46}^* = \dot{x}_{13}^d - K_1(x_{13} - x_{13}^d) \tag{40}$$

Matrix $K_1 \in R^{3\times3}$ is a diagonal matrix, where its diagonal elements $k_{i1} > 0, \ i = 1,2,3$. For the subsystem of Eq. (37), the control inputs vector $u$ is selected so as to ensure that $x_{46}$ will converge to the targeted value $x_{46}^*$ which makes the state vector of the subsystem of Eq. (36) converge to the associated setpoint. Thus the setpoint for the subsystem of Eq. (37) is $x_{46}^d = x_{46}^*$ and control input $u$ is given by

$$u = g_{46}(x)^{-1}[\dot{x}_{46}^d - f_{46}(x) - K_2(x_{46} - x_{46}^d)] \tag{41}$$

Matrix $K_2 \in R^{3\times3}$ is a diagonal matrix, where its diagonal elements $k_{i1} > 0, \ i = 1,2,3$. By substituting Eq. (40) into Eq. (36), as well as by substituting Eq. (41) into Eq. (37) one obtains the following closed-loop system dynamics

$$(\dot{x}_{13} - \dot{x}_{13}^d) + K_1(x_{13} - x_{13}^d) = 0 \tag{42}$$

$$(\dot{x}_{46} - \dot{x}_{46}^d) + K_2(x_{46} - x_{46}^d) = 0 \tag{43}$$

Next, by defining the tracking error variables $e_{13} = x_{13} - x_{13}^d$ and $e_{46} = x_{46} - x_{46}^d$ one has that

$$\begin{array}{c} \dot{e}_{13} + K_1 e_{13} = 0 \Rightarrow lim_{t\to\infty} e_{13} = 0 \Rightarrow lim_{t\to\infty} x_{13}(t) = x_{13}^d(t) \\ \dot{e}_{46} + K_2 e_{46} = 0 \Rightarrow lim_{t\to\infty} e_{46} = 0 \Rightarrow lim_{t\to\infty} x_{46}(t) = x_{46}^d(t) \end{array} \tag{44}$$

Consequently, all state variables of the redundant robotic manipulator converge to the associated setpoints, or $lim_{t\to\infty} x_i(t) = x_i^d(t)$, for $i = 1,2,\cdots,6$.

The global stability properties of the control scheme can be also proven through Lyapunov analysis. The following Lyapunov function is defined

$$V = \frac{1}{2}[e_{13}^T e_{13} + e_{46}^T e_{46}] \tag{45}$$

By differentiating the above Lyapunov function in time

$$\begin{array}{c} \dot{V} = e_{13}^T \dot{e}_{13} + e_{46}^T \dot{e}_{46} \Rightarrow \dot{V} = e_{13}^T(-K_1 e_{13} + e_{46}^T(-K_2 e_{46}) \\ \Rightarrow \dot{V} = -K_1 e_{13}^T e_{13} - K_2 e_{46}^T e_{46} \Rightarrow \dot{V} < 0 \end{array} \tag{46}$$

Thus it holds that $\dot{V}$ is strictly negative $\forall \ e_{13} \neq 0, e_{46} \neq 0$ while it becomes 0 only when $e_{13} = 0$, $e_{46} = 0$. Consequently, the above given Lyapunov function $V$ is a positive and strictly diminishing function which, no matter what its initial value is, approaches asymptotically the equilibrium $(e_{13}^T, e_{46}^T) = (0_{1\times3}, 0_{1\times3})$. As a result of the above, flatness-based control in successive loops for the 3-DOF redundant robotic manipulator, ensures global asymptotic stability.

# 4 Flatness-based control in successive loops for 3-DOF autonomous underwater vessels

## 4.1 Dynamic model of the 3-DOF autonomous underwater vessel

The second test case for the flatness-based control approach in successive loops is concerned with Autonomous Underwater Vessels (AUVs). The use of Autonomous Underwater Vessels (AUVs) is widely met in defense and security tasks, in missions for seabed exploration and exploitation, in the construction of underwater pipelines and in the birthing of underwater cables, as well in scientific exploration missions [2]. The kinematic and dynamic model of these robotic systems is a strongly nonlinear one and receives multiple control inputs in the form of thrust forces from the AUVs' propulsion system [41-45]. Depending on whether the number of degrees of freedom of such AUVs exceeds the number of their control inputs or not, AUVs can be classified into underactuated and fully actuated ones [46 -49]. The control problem of

AUVs is a non-trivial one and several nonlinear control methods have been proposed for it so far [50-54]. Precise path following under model uncertainty and external perturbations is the main objectives of these control schemes [55-59]. Besides, minimization in energy consumption by the electric actuators of AUVs is another significant research target. To this end, MPC and NMPC control methods can be considered [60-63].

The diagram of the 3-DOF autonomous underwater vessel is shown in Fig. 2. The joint kinematic and dynamic model of the 3-DOF autonomous underwater vessel is [3]

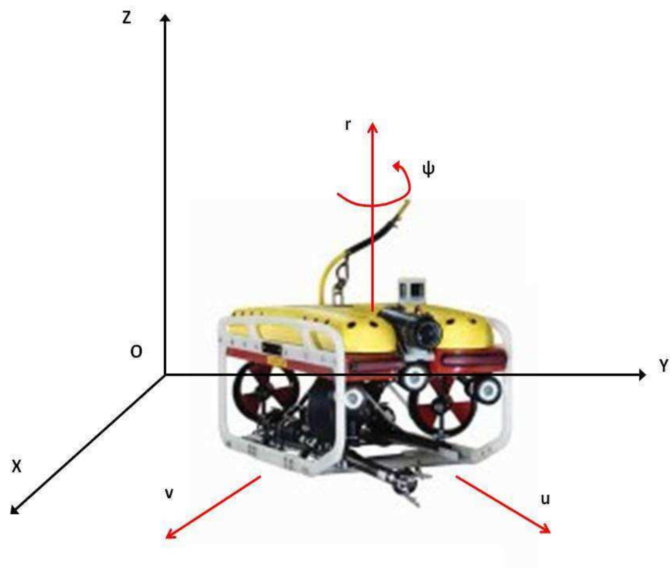


Figure 2: Diagram of the 3-DOF autonomous underwater vessel and of the associated body-fixed and inertial reference frames

$$\begin{array}{c} \dot{x} = ucos(\psi) - vsin(\psi) \\ \dot{y} = usin(\psi) + vcos(\psi) \\ \dot{\psi} = r \\ \dot{u} = \frac{M_{\dot{v}}}{M_{\dot{u}}} v \cdot r - \frac{X_u}{M_{\dot{u}}} u - \frac{D_u}{M_{\dot{u}}} u|u| + \frac{1}{M_{\dot{u}}} F_u \\ \dot{v} = -\frac{M_{\dot{u}}}{M_{\dot{v}}} u \cdot r - \frac{Y_u}{M_{\dot{v}}} v - \frac{D_v}{M_{\dot{v}}} v|v| + \frac{1}{M_{\dot{v}}} F_v \\ \dot{r} = \frac{M_{\dot{u}} - M_{\dot{v}}}{M_{\dot{r}}} u \cdot v - \frac{N_r}{M_r} r - \frac{D_r}{M_r} r|r| + \frac{1}{M_r} F_r \end{array} \quad (47)$$

By defining the state vector $x = [x_1, x_2, x_3, x_4, x_5, x_6]^T = [x, y, \psi, u, v, r]^T$ the kinematic-dynamic model of the AUV can be written in the following matrix form:

$$\begin{pmatrix} \dot{x}_1 \\ \dot{x}_2 \\ \dot{x}_3 \\ \dot{x}_4 \\ \dot{x}_5 \\ \dot{x}_6 \end{pmatrix} = \begin{pmatrix} x_4 cos(x_3) - x_5 sin(x_3) \\ x_4 sin(x_3) + x_5 cos(x_3) \\ x_6 \\ \frac{M_{\dot{x}_5}}{M_{\dot{u}}} x_5 \cdot x_6 - \frac{X_u}{M_{\dot{u}}} x_4 - \frac{D_u}{M_{\dot{u}}} x_6|x_6| \\ -\frac{M_{\dot{u}}}{M_{\dot{v}}} u \cdot r - \frac{Y_u}{M_{\dot{v}}} x_5 - \frac{D_v}{M_{\dot{v}}} x_5|x_5| \\ \frac{M_{\dot{u}} - M_{\dot{v}}}{M_{\dot{r}}} x_4 \cdot x_5 - \frac{N_r}{M_r} x_6 - \frac{D_r}{M_r} x_6|x_6| \end{pmatrix} + \begin{pmatrix} 0 & 0 & 0 \\ 0 & 0 & 0 \\ 0 & 0 & 0 \\ \frac{1}{M_{\dot{u}}} & 0 & 0 \\ 0 & \frac{1}{M_{\dot{v}}} & 0 \\ 0 & 0 & \frac{1}{M_{\dot{r}}} \end{pmatrix} \begin{pmatrix} u_1 \\ u_2 \\ u_3 \end{pmatrix} \quad (48)$$

The following state variables are defined: $x_{13} = [x_1, x_2, x_3]^T$, $x_{46} = [x_4, x_5, x_6]^T$. The following vectors and matrices are also defined

$$f_{13} = \begin{pmatrix} x_4 cos(x_3) - x_5 sin(x_3) \\ x_4 sin(x_3) + x_5 cos(x_3) \\ x_6 \end{pmatrix} \quad f_{46} = \begin{pmatrix} \frac{M_{\dot{x}_5}}{M_{\dot{u}}} x_5 \cdot x_6 - \frac{X_u}{M_{\dot{u}}} x_4 - \frac{D_u}{M_{\dot{u}}} x_6 |x_6| \\ -\frac{M_{\dot{u}}}{M_{\dot{v}}} u \cdot r - \frac{Y_u}{M_{\dot{v}}} x_5 - \frac{D_v}{M_{\dot{v}}} x_5 |x_5| \\ \frac{M_{\dot{u}} - M_{\dot{v}}}{M_{\dot{r}}} x_4 \cdot x_5 - \frac{N_r}{M_r} x_6 - \frac{D_r}{M_r} x_6 |x_6| \end{pmatrix} \tag{49}$$

$$R_{13} = \begin{pmatrix} cos(x_3) & -sin(x_3) & 0 \\ sin(x_3) & cos(x_3) & 0 \\ 0 & 0 & 1 \end{pmatrix} \quad g_{46} = \begin{pmatrix} \frac{1}{M_{\dot{u}}} & 0 & 0 \\ 0 & \frac{1}{M_{\dot{v}}} & 0 \\ 0 & 0 & \frac{1}{M_{\dot{r}}} \end{pmatrix} \tag{50}$$

Consequently, the kinematic-dynamic model of the AUV can be decomposed into two subsystems

$$\dot{x}_{13} = R_{13} x_{46} \tag{51}$$

$$\dot{x}_{46} = f_{46}(x) + g_{46}(x) u \tag{52}$$

It can be proven that $y = x_{13}$ is a flat output for the AUV's model defined in the subsystems of Eq. (51) and Eq. (52). From Eq. (51) one has

$$\begin{matrix} \dot{x}_{13} = R_{13} x_{46} \Rightarrow x_{46} = R_{13}^{-1} \dot{x}_{13} \\ Rightarrow x_{46} = R_{13}^{-1}(y) \dot{y} \end{matrix} \tag{53}$$

where $R_{13}$ is a function of only $x_{13}$, thus $x_{46}$ is a differential function of the flat output $y$. From Eq. (52), using that $f_{46}(x)$ and $g_{46}(x)$ are functions of $x_{46}$ and finally of the flat output $y$ and also that

$$u = g_{46}(x)^{-1} [\dot{x}_{46} - f_{46}(x)] \tag{54}$$

this signifies that $u$ is a differential function of the flat output $y$. Consequently, the system of Eq. (51) and Eq. (52) is differentially flat.

### 4.2 Flatness-based controller in successive loops for 3-DOF AUVs

Besides, it can be demonstrated that each one of the independent subsystems of Eq. (51) and Eq. (52) is differentially flat. In Eq. (51) $x_{46}$ is considered to be a virtual control input and $x_{13}$ is taken to be the flat output of this subsystem. Thus,

$$x_{46} = R_{13}^{-1} \dot{x}_{13} \tag{55}$$

which signifies that the virtual control input $x_{46}$ is a differential function of the flat output $x_{13}$. Thus the subsystem of Eq. (51) is differentially flat.

In Eq. (52) $x_{46}$ is considered to be a flat output and $f_{46}(x)$, $g_{46}(x)$ are functions of $x_{46}$. By considering that that $f_{46}(x)$ and $g_{46}(x)$ are functions of $x_{46}$ and solving for control input $u$ as in Eq. (54) it is demonstrated again that $u$ is a differential function of the flat output $x_{46}$. Thus, the subsystem of Eq. (52) is also differentially flat.

Next, one can solve the control problem for the individual subsystems of Eq. (51) and Eq. (52) using the stages of controller for input-output linearized differentially flat systems. For, the subsystem of Eq. (51), the value of the virtual control input $x_{46}$ which stabilizes the system's dynamics is

$$x_{46}^* = R_{13}^{-1} [\dot{x}_{13}^d - K_1(x_{13} - x_{13}^d)] \tag{56}$$

where $K_1 \in R^{3\times3}$ is a diagonal matrix with diagonal elements $k_{i1} > 0,\ i = 1, 2, 3$. For the subsystem of Eq. (52), the targeted setpoint is the one that assures the stabilization and elimination of tracking error for the first subsystem, that is $x_{46}^d = x_{46}^*$. The value of the control input $u$ which assures convergence of $x_{46}$ to $x_{46}^d$ is

$$u = g_{46}^{-1}[\dot{x}_{46}^d - f_{46}(x) - K_2(x_{46} - x_{46}^d)] \tag{57}$$

By substituting Eq. (56) into Eq. (51), as well as Eq. (57) into Eq. (52) the following closed-loop system dynamics is obtained for the above-noted subsystems

$$\begin{array}{c} (\dot{x}_{13} - \dot{x}_{13}^d) + K_1(x_{13} - x_{13}^d) = 0 \\ (\dot{x}_{46} - \dot{x}_{46}^d) + K_2(x_{46} - x_{46}^d) = 0 \end{array} \tag{58}$$

Moreover, by defining the tracking error variables $e_{13} = x_{13} - x_{13}^d$ and $e_{46} = x_{46} - x_{46}^d$ one has that

$$\begin{array}{c} \dot{e}_{13} + K_1 e_{13} = 0 \Rightarrow lim_{t\to\infty} e_{13} = 0 \Rightarrow lim_{t\to\infty} x_{13}(t) = x_{13}^d(t) \\ \dot{e}_{46} + K_2 e_{46} = 0 \Rightarrow lim_{t\to\infty} e_{46} = 0 \Rightarrow lim_{t\to\infty} x_{46}(t) = x_{46}^d(t) \end{array} \tag{59}$$

Consequently, all state variables of the 3-DOF AUV converge to the associated setpoints, or $lim_{t\to\infty} x_i(t) = x_i^d(t)$, for $i = 1, 2, \cdots, 6$.

The global stability properties of the control scheme can be also proven through Lyapunov analysis. The following Lyapunov function is defined

$$V = \frac{1}{2}[e_{13}^T e_{13} + e_{46}^T e_{46}] \tag{60}$$

By differentiating the above Lyapunov function in time

$$\begin{array}{c} \dot{V} = e_{13}^T \dot{e}_{13} + e_{46}^T \dot{e}_{46} \Rightarrow \dot{V} = e_{13}^T(-K_1 e_{13} + e_{46}^T(-K_2 e_{46}) \\ \Rightarrow \dot{V} = -K_1 e_{13}^T e_{13} - K_2 e_{46}^T e_{46} \Rightarrow \dot{V} < 0 \end{array} \tag{61}$$

Thus it holds that $\dot{V}$ is strictly negative $\forall$ $e_{13} \neq 0, e_{46} \neq 0$ while it becomes 0 only when $e_{13} = 0$, $e_{46}$. Consequently, the above given Lyapunov function $V$ is a positive and strictly diminishing function which, no matter what its initial value is, approaches asymptotically the equilibrium $(e_{13}^T, e_{46}^T) = (0_{1\times 3}, 0_{1\times 3})$. As a result of the above, flatness-based control in successive loops for the 3-DOF AUV, ensures global asymptotic stability.

## 5 Simulation tests

### 5.1 Control of the 3-DOF redundant robotic manipulator

Results about the tracking accuracy and the speed of convergence to setpoints of the successive-loops flatness-based control method, in the case of the 3-DOF redundant robotic manipulator, are shown in Fig. 3 to Fig. 10. It can be noticed, that under this control scheme one achieves fast and precise tracking of reference setpoints for all state variables of the robotic system. It is noteworthy, that through the stages of this method one solves also the setpoints definition problem for all state variables of the redundant robotic manipulator. Actually, the selection of setpoints for state variables $x_1$, $x_2$ and $x_3$ is unconstrained. On the other side by defining state variables $x_4$, $x_5$ and $x_4$ as virtual control inputs for the subsystem of $x_1$, $x_2$ and $x_3$ one can find the setpoints for $x_4$, $x_5$, $x_6$ as functions of the setpoints for $x_1$, $x_2$, $x_3$. The speed of convergence of the state variables of the robotic system under flatness-based control implemented in successive loops is dependent on the selection of values for the diagonal gain matrices $K_1$, $K_2$ of Eq. (40) and Eq. (41).

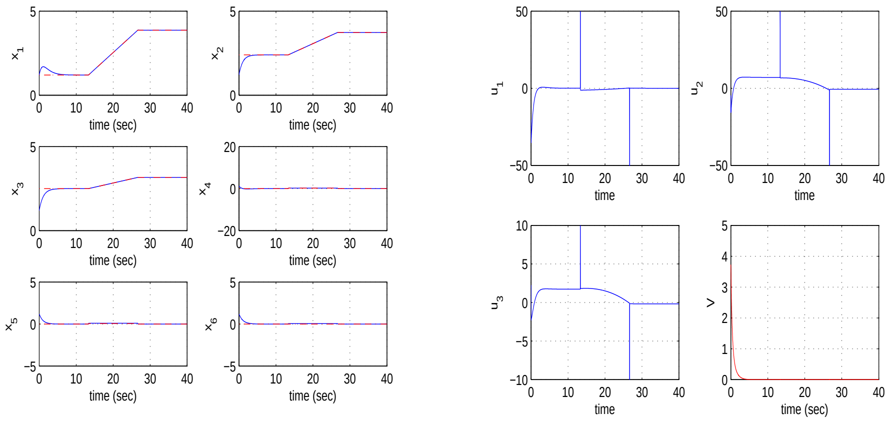


**(a)** **(b)**

Figure 3: Tracking of trajectory 1 by the 3-DOF redundant robotic manipulator (a) convergence of state variables $x_1$ to $x_6$ to their reference setpoints (red line: setpoint, blue line: real value), (b) variation of control inputs $u_1$ to $u_3$ (blue lines) and Lyapunov function $V$ (red line)

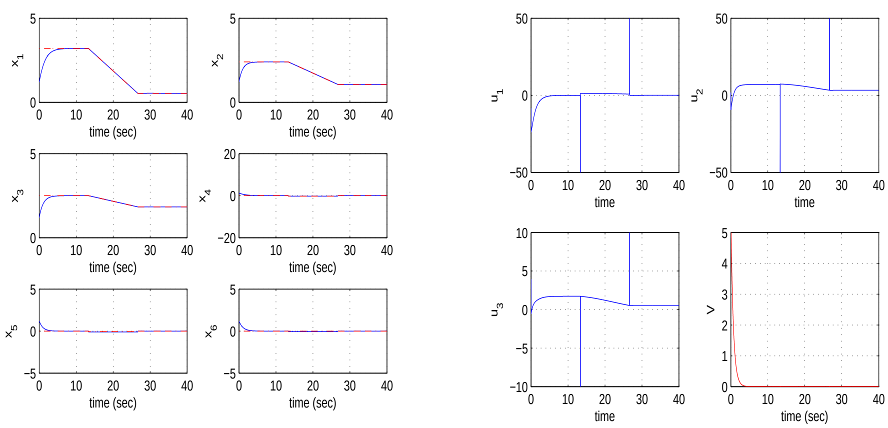


**(a)** **(b)**

Figure 4: Tracking of trajectory 2 by the 3-DOF redundant robotic manipulator (a) convergence of state variables $x_1$ to $x_6$ to their reference setpoints (red line: setpoint, blue line: real value), (b) variation of control inputs $u_1$ to $u_3$ (blue lines) and Lyapunov function $V$ (red line) (red line)

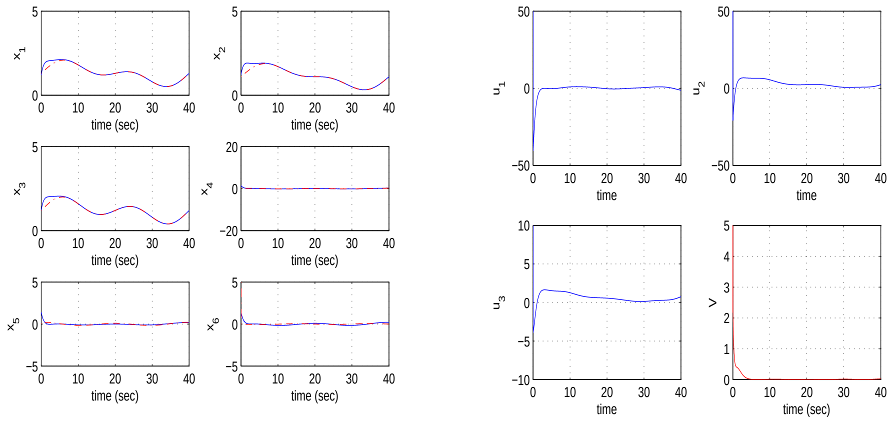


**(a)** **(b)**

Figure 5: Tracking of trajectory 3 by the 3-DOF redundant robotic manipulator (a) convergence of state variables $x_1$ to $x_6$ to their reference setpoints (red line: setpoint, blue line: real value), (b) variation of control inputs $u_1$ to $u_3$ (blue lines) and Lyapunov function $V$ (red line) (red line)

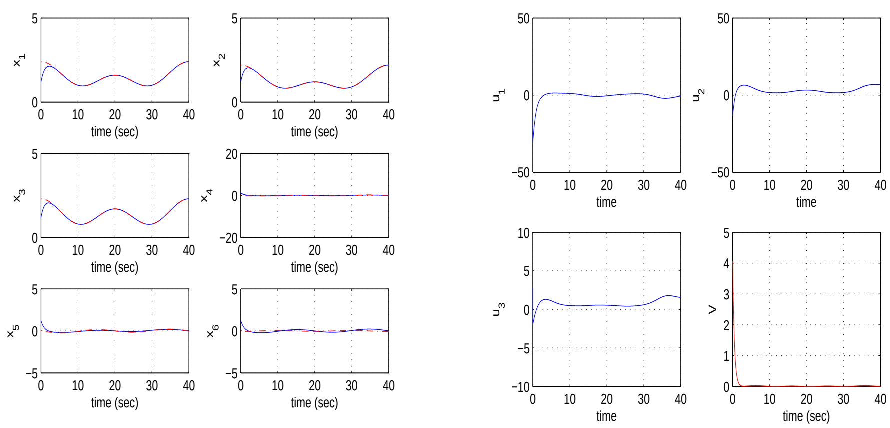


**(a)** **(b)**

Figure 6: Tracking of trajectory 4 by the 3-DOF redundant robotic manipulator (a) convergence of state variables $x_1$ to $x_6$ to their reference setpoints (red line: setpoint, blue line: real value), (b) variation of control inputs $u_1$ to $u_3$ (blue lines) and and Lyapunov function $V$ (red line) (red line)

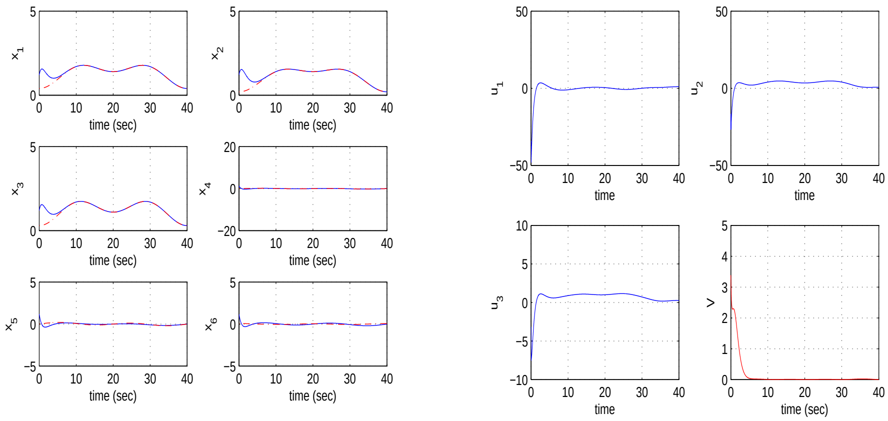


**(a)** **(b)**

Figure 7: Tracking of trajectory 5 by the 3-DOF redundant robotic manipulator (a) convergence of state variables $x_1$ to $x_6$ to their reference setpoints (red line: setpoint, blue line: real value), (b) variation of control inputs $u_1$ to $u_3$ (blue lines) and Lyapunov function $V$ (red line) (red line)

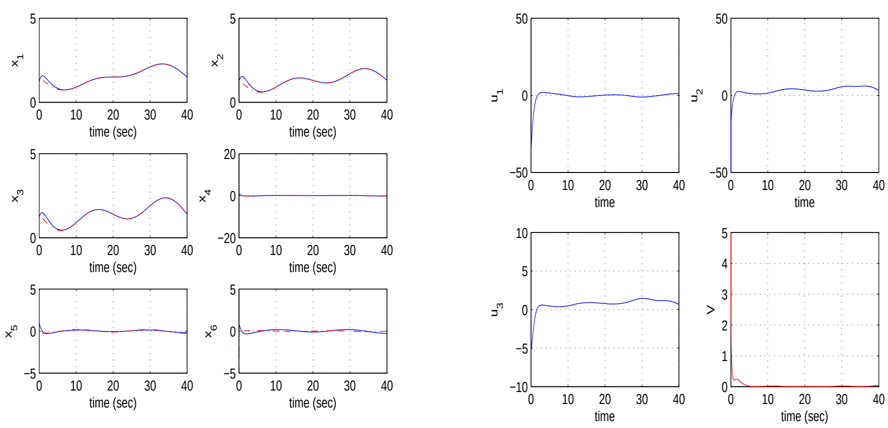


**(a)** **(b)**

Figure 8: Tracking of trajectory 6 by the 3-DOF redundant robotic manipulator (a) convergence of state variables $x_1$ to $x_6$ to their reference setpoints (red line: setpoint, blue line: real value), (b) variation of control inputs $u_1$ to $u_3$ (blue lines) and Lyapunov function $V$ (red line) (red line)

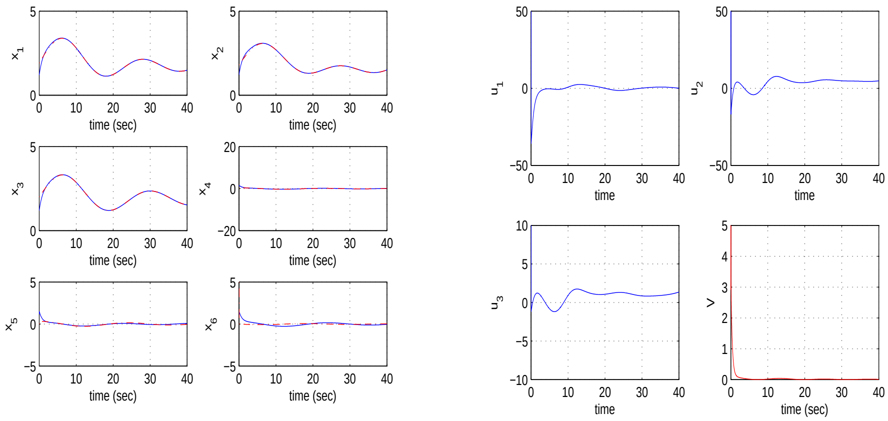



**(a)** **(b)**

Figure 9: Tracking of trajectory 7 by the 3-DOF redundant robotic manipulator (a) convergence of state variables $x_1$ to $x_6$ to their reference setpoints (red line: setpoint, blue line: real value), (b) variation of control inputs $u_1$ to $u_3$ (blue lines) and Lyapunov function $V$ (red line) (red line)

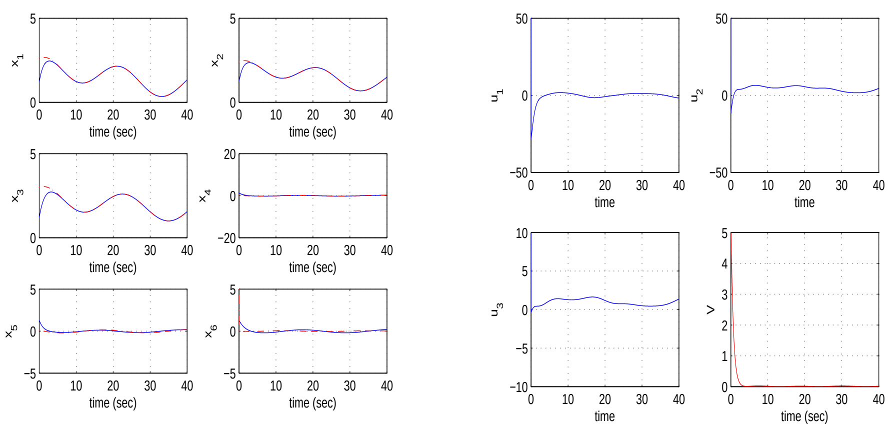



**(a)** **(b)**

Figure 10: Tracking of trajectory 8 by the 3-DOF redundant robotic manipulator (a) convergence of state variables $x_1$ to $x_6$ to their reference setpoints (red line: setpoint, blue line: real value), (b) variation of control inputs $u_1$ to $u_3$ (blue lines) and Lyapunov function $V$ (red line) (red line)

### 5.2 Control of the 3-DOF autonomous underwater vessel

Results about the tracking accuracy and the speed of convergence to setpoints of the successive-loops flatness-based control method, in the case of the 3-DOF autonomous underwater vessel, are shown in Fig. 11 to Fig. 18. It can be noticed again, that under this control scheme one achieves fast and precise tracking of reference setpoints for all state variables of the autonomous underwater vessel. It is noteworthy, that through the stages of this method one solves also the setpoints definition problem for all state variables of the AUV. Actually, the selection of setpoints for state variables $x_1$, $x_2$ and $x_3$ is unconstrained. On the other side by defining state variables $x_4$, $x_5$ and $x_4$ as virtual control inputs for the subsystem of $x_1$, $x_2$ and $x_3$ one can find the setpoints for $x_4$, $x_5$, $x_6$ as functions of the setpoints for $x_1$, $x_2$, $x_3$. The speed of convergence of the state variables of the autonomous underwater vessel under flatness-based control implemented in successive loops is dependent on the selection of values for the diagonal gain matrices $K_1$, $K_2$ of Eq. (56) and Eq. (57).

## 6 Conclusions

The paper has introduced and analyzed a new approach for the control of nonlinear dynamical systems, based on differential flatness theory. The method is directly applicable to systems with a state-space model in the so-called triangular form, or can be used in systems which can be transformed to the triangular form after a change of variables. In the proposed controller design method each subsystem of the state-space model of the nonlinear system is shown to be differentially flat, while the associated state variable is taken to be the flat output. Next, a virtual control input is computed for each subsystem of the state-space model. The virtual control input can invert the subsystem's dynamics while also eliminating the subsystem's tracking error. The control input that is actually applied to the nonlinear system is computed from the last subsystem of the state-space description. This control input contains recursively all virtual control inputs which were found for the individual subsystems of the state-space equation. Thus, at each iteration of the control algorithm and by tracing the subsystems of the state-space model backwards, one can finally obtain the control input that should be applied to the nonlinear system so as to assure that all its state vector elements will converge to the desirable setpoints.

As a case study, the control problem for the multivariable and nonlinear dynamics of robotic manipulators and autonomous vehicles has been solved with the use of the flatness-based control approach which is implemented in successive loops. The state-space model of these robotic systems is separated into two subsystems, which are connected between them in cascading loops. Each one of these subsystems can be viewed independently as a differentially flat system and control about it can be performed with inversion of its dynamics as in the case of input-output linearized flat systems. The state variables of the second subsystem become virtual control inputs for the first subsystem. In turn exogenous control inputs are applied to the first subsystem. The whole control method is implemented in two successive loops and its global stability properties are also proven through Lyapunov stability analysis. The fine performance of the control method is confirmed in two case studies: (a) control of a 3-DOF redundant rigid-link robotic manipulator, (ii) control of a 3-DOF autonomous underwater vessel.

## References

[1] G. Rigatos, Nonlinear control and filtering using differential flatnesss theory approaches: Applications to electromechanical systems, Springer, 2016

[2] G. Rigatos and K. Busawon, Robotic manipulators and vehicles: Control, estimation and filtering, Springer, 2018

[3] G. Rigatos, M. Abbaszadeh, P. Siano, Control and estimation of dynamical nonlinear and partial differential equation systems: Theory and Applications, IET Publications, 2022

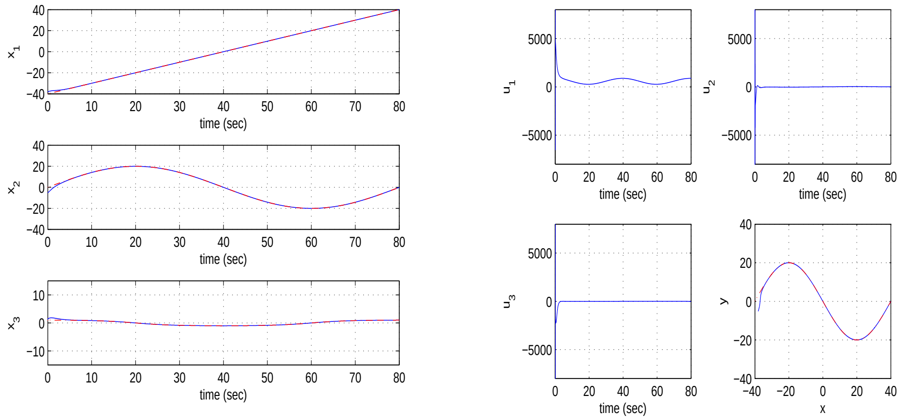


**(a)** **(b)**

Figure 11: Tracking of trajectory 1 by the 3-DOF autonomous underwater vessel (a) convergence of state variables $x_1$ to $x_6$ to their reference setpoints (red line: setpoint, blue line: real value), (b) variation of control inputs $u_1$ to $u_3$ (blue lines) and position $(x_p, y_p)$ of the AUV on the xy plane (blue line) vs desirable position (red line)

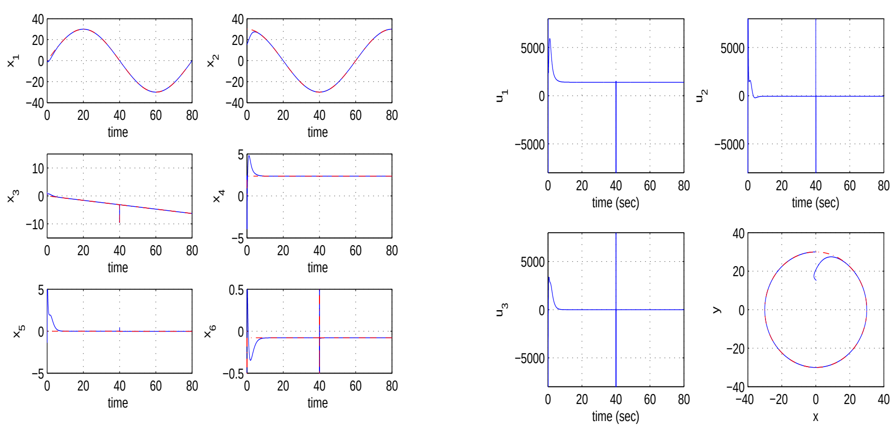


**(a)** **(b)**

Figure 12: Tracking of trajectory 2 by the 3-DOF autonomous underwater vessel (a) convergence of state variables $x_1$ to $x_6$ to their reference setpoints (red line: setpoint, blue line: real value), (b) variation of control inputs $u_1$ to $u_3$ (blue lines) and position $(x_p, y_p)$ of the AUV on the xy plane (blue line) vs desirable position (red line)

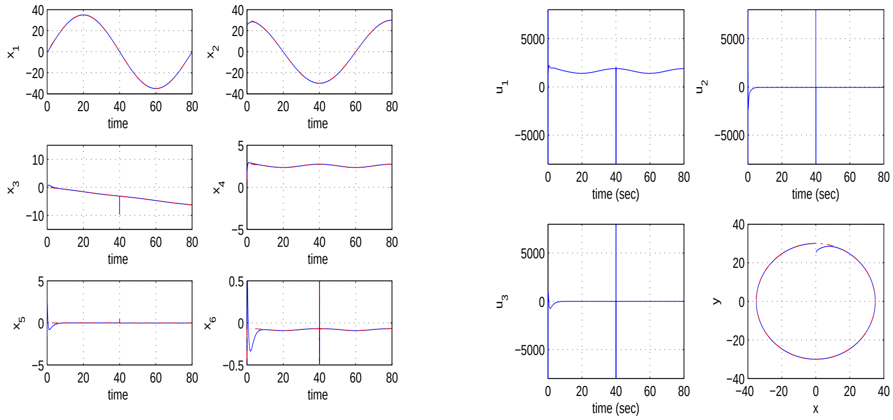


**(a)** **(b)**

Figure 13: Tracking of trajectory 3 by the 3-DOF autonomous underwater vessel (a) convergence of state variables $x_1$ to $x_6$ to their reference setpoints (red line: setpoint, blue line: real value), (b) variation of control inputs $u_1$ to $u_3$ (blue lines) and position $(x_p, y_p)$ of the AUV on the xy plane (blue line) vs desirable position (red line)

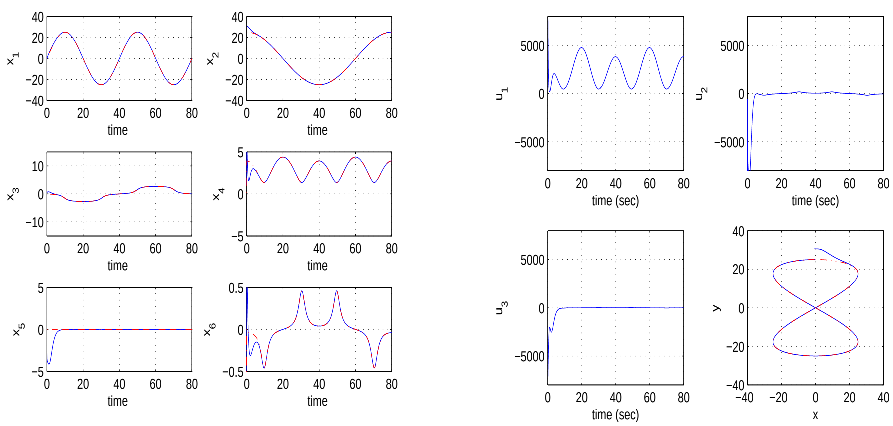


**(a)** **(b)**

Figure 14: Tracking of trajectory 4 by the 3-DOF autonomous underwater vessel (a) convergence of state variables $x_1$ to $x_6$ to their reference setpoints (red line: setpoint, blue line: real value), (b) variation of control inputs $u_1$ to $u_3$ (blue lines) and position $(x_p, y_p)$ of the AUV on the xy plane (blue line) vs desirable position (red line)

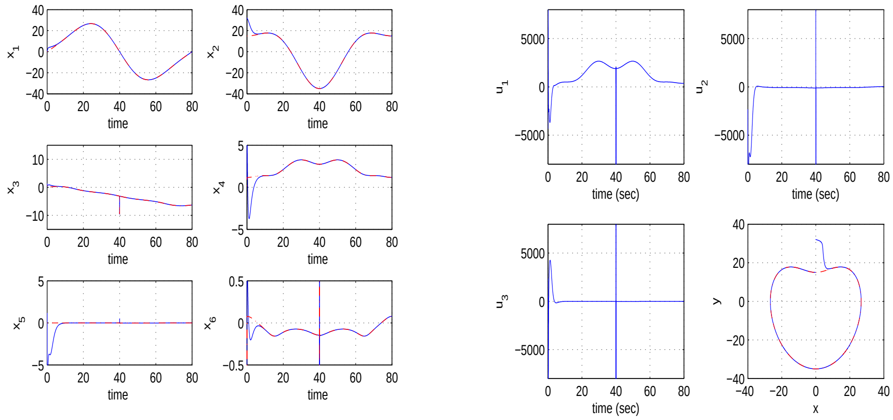


**(a)** **(b)**

Figure 15: Tracking of trajectory 5 by the 3-DOF autonomous underwater vessel (a) convergence of state variables $x_1$ to $x_6$ to their reference setpoints (red line: setpoint, blue line: real value), (b) variation of control inputs $u_1$ to $u_3$ (blue lines) and position $(x_p, y_p)$ of the AUV on the xy plane (blue line) vs desirable position (red line)

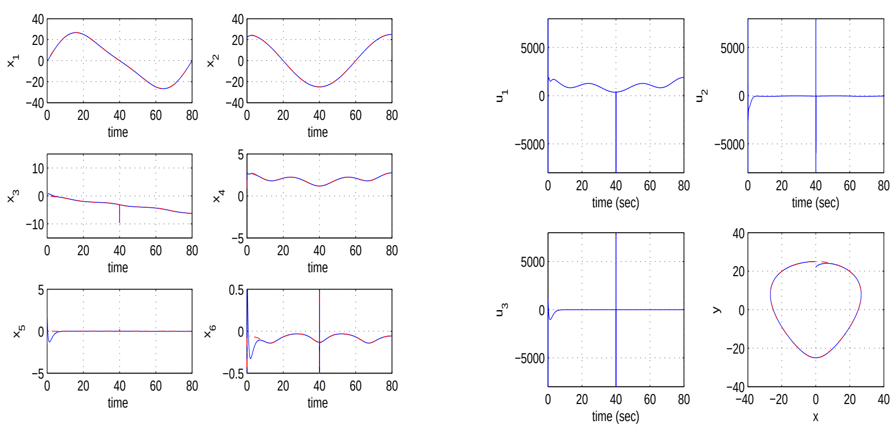


**(a)** **(b)**

Figure 16: Tracking of trajectory 6 by the 3-DOF autonomous underwater vessel (a) convergence of state variables $x_1$ to $x_6$ to their reference setpoints (red line: setpoint, blue line: real value), (b) variation of control inputs $u_1$ to $u_3$ (blue lines) and position $(x_p, y_p)$ of the AUV on the xy plane (blue line) vs desirable position (red line)

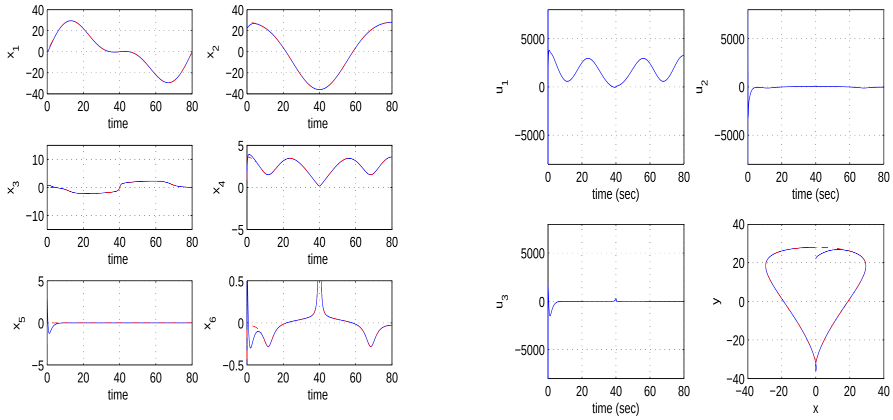


**(a)** **(b)**

Figure 17: Tracking of trajectory 7 by the 3-DOF autonomous underwater vessel (a) convergence of state variables $x_1$ to $x_6$ to their reference setpoints (red line: setpoint, blue line: real value), (b) variation of control inputs $u_1$ to $u_3$ (blue lines) and position $(x_p, y_p)$ of the AUV on the xy plane (blue line) vs desirable position (red line)

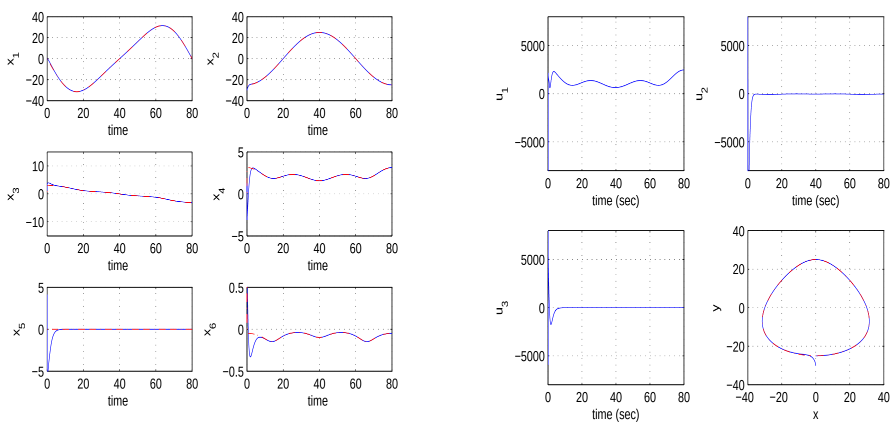


**(a)** **(b)**

Figure 18: Tracking of trajectory 8 by the 3-DOF autonomous underwater vessel (a) convergence of state variables $x_1$ to $x_6$ to their reference setpoints (red line: setpoint, blue line: real value), (b) variation of control inputs $u_1$ to $u_3$ (blue lines) and position $(x_p, y_p)$ of the AUV on the xy plane (blue line) vs desirable position (red line)

[4] J.Levine, Analysis and Control of Nonlinear Systems: A flatness-based approach, Springer 2009.

[5] M. Fliess and H. Mounier, Tracking control and $\pi$-freeness of infinite dimensional linear systems, In: G. Picci and D.S. Gilliam Eds.,Dynamical Systems, Control, Coding and Computer Vision, vol. 258, pp. 41-68, *Birkhaüser*, 1999.

[6] J. Villagra, B. d'Andrea-Novel, H. Mounier and M. Pengov, Flatness-based vehicle steering control strategy with SDRE feedback gains tuned via a sensitivity approach, IEEE Transactions on Control Systems Technology, vol. 15, pp. 554- 565, 2007.

[7] S. Bououden, D. Boutat, G. Zheng, J.P. Barbot and F. Kratz, A triangular canonical form for a class of 0-flat nonlinear systems, International Journal of Control, Taylor and Francis, vol. 84, no. 2, pp. 261-269, 2011.

[8] L. Menhour, B. d'Andre'a-Novel, M. Fliess and H. Mounier, Coupled nonlinear vehicle control: Flatness-based setting with algebraic estimation techniques, Control Engineering Practice, Elsevier, vol. 22, pp. 135–146, 2014

[9] F. Nicolaum W. Respondek and J.P. Barbot, How to minimally modify a dynamical system when constructing flat inputs, Internattional Journal of Robust and Nonlinear Control, J. Wiley, 2022.

[10] C. Letelier nd J.P. Barbot, Optimal flatness placement of sensors and actuators for controlling chaotic systemsm Chaos, AIP Publications, vol. 31, no. 10, article No 103114, 2021.

[11] H. Sira-Ramirez and S. Agrawal, Differentially Flat Systems, Marcel Dekker, New York, 2004.

[12] J. Lévine, On necessary and sufficient conditions for differential flatness, Applicable Algebra in Engineering, Communications and Computing, Springer, vol. 22, no. 1, pp. 47-90, 2011.

[13] F. Nicolau, W. Respondek and J.P. Barbot, Construction of flat inputs for mechanical systems, 7th IFAC Workshop on Lagrangian and Hamiltonian methods for nonlinear control, Berlin, Germany, OCt. 2021

[14] J.O. Limaverde Filho, E.C.R. Fortaleza and M.C.M. Campos, A derivative-free nonlinear Kalman Filtering approach using flat inputs, International Journal of Control, Taylor and Francis 2021.

[15] J.P. Barbot, M. Fliess and T. Floquet, An algebraic framework for the design of nonlinear observers with uknown inputs, IEEE CDC 2007, IEEE 46th Intl. Conference on Decision and Control, New Orleans, USA, Dec. 2007

[16] H. Khalil, Nonlinear Systems, Prentice Hall, 1996

[17] G.G. Rigatos and S.G. Tzafestas, Extended Kalman Filtering for Fuzzy Modelling and Multi-Sensor Fusion, Mathematical and Computer Modelling of Dynamical Systems, Taylor & Francis), vol. 13, pp. 251-266, 2007.

[18] M. Basseville and I. Nikiforov, Detection of abrupt changes: Theory and Applications, *Prentice-Hall*, 1993.

[19] G. Rigatos and Q. Zhang, Fuzzy model validation using the local statistical approach, Fuzzy Sets and Systems, Elsevier, vol. 60, no. 7, pp. 882-904,2009.

[20] G. Rigatos, P. Siano and N. Zervos, A new concept of flatness-based control of nonlinear dynamical systems, IEEE INDIN 2015, 13th IEEE Intl. Conf. on Industrial Informatics, Cambridge, UK, July 2015

[21] G. Rigatos, P. Siano, S Ademi and P. Wira, Flatness-based control of DC-DC converters implemented in successive loops, Electric Power Components and Systems, Taylor and Francis, vol. 46, no. 6, pp. 673-687, 2018.

[22] G. Rigatos, Flatness-based embedded control in successive loops for spark ignited engines, Journal of Physics, IOP Publications, Conference Series No 659, 012019, IFAC ACD 2015, Proc. of the 12th European Workshop on Advanced Control and Diagnosis.

[23] G. Rigatos and A. Melkikh, Flatness-based control in successive loops for stabilization of heart's electrical activity, In Proc. ICNAAM 2016, AIP Conf. Proceedings No 1790 060004, Intl. Conf. on Numerical Analysis and Applied Mathematics, 2016

[24] G. Rigatos and P. Siano, Flatness-based control in successive loops for Business Cycles of Finance Agents, Journal of Intelligent Industrial Systems, Springer, vol. 3, pp. 77-89, 2017

[25] D. Nicolis, F. Allewi and P. Rocco, Operational space model predictive sliding-mode control for redundant manipulators, IEEE Transactions on Robotics, pp. 1-10, 2020.

[26] J. Jin and Y. Zhang, G2-type SRMPC scheme for synchronous manipulation of two redundant robot arms, IEEE Transactions on Cybernetics, vol. 45, no. 2, pp. 153-164, 2015.

[27] M. Galicki, Path-constrained control of a redundant manipulator in a task space, Robotics and Autonomous Systems, Elsevier, vol. 34, pp. 234-243, 2006.

[28] P. Jiang, S. Huang, J. Xiang and M.Z.Q. Chen, Iteratively successive projection: A novel continuoous approach for the task-based control of redundant robots, IEEE Access, vo.. 7, pp. 25347-25358, 2019.

[29] G. Oriolo, M. Cefalo and M. Venditelli, Repeatable motion planning for redunant robots over cyclic tasks, IEEE Transactions on Robotics, vol. 33, no. 5, pp. 1170-1187, 2017.

[30] S. Kayastha, L. Shi, J. Katapitiya and G. Pearce, Nonlinear Model Predictive Control of a planar three-link space manipulator, IEEE ASCC 2017, 11th Asian Control Conference, Gold Coast, Australia, Dec. 2017

[31] N. Kumar, V. Panwar, N. Sukovanam, S.P. Sharma and J.H. Borm, Neural network-based nonlinear tracking control of kinematically redundant robot manipulator, Mathematics and Computer Modelling, Elsevier, vol. 57, pp. 1889-1901, 2001.

[32] J. Sandeval, P. Vieyes and G. Poisson. Generalized framework for control of redundant manipulators in robot-assisted minimal invasive surgery, IRBM Journal (Innovation and Research in Biomedical Engineering), Elsevier, vol. 39, pp. 160-166, 2018.

[33] V. Potkonjak, M. Popovic, M. Lazarevic and J. Sinanovic, Redundancy problem in writing: from human to anthropomorphic robot arm, IEEE Transactions on Systems, Man and Cybernetics - Part B: Cybernetics, vol. 28, no. 6, pp. 790-805, 1998.

[34] Z. Wang, B. Wang, L. Xu and Q. Xie, Feedback-added pseudoinverse type balanced minimization scheme for kinematic control of redundant robot manipulators, IEEE Access, vol. 7, pp. 23806-23815, 2017.

[35] A.M. Jassour and M. Farrokhi, Adaptive neuropredictive control for redundant robot manipulators in presence of static and dynamic obstacles: A Lyapunov-based approach, Intl. Journal of Adaptive Control and Signal Processing, vol. 28, no. 3-5, pp. 386-411, 2014.

[36] B. Xian, M.S. de Queiroz, D. Dawson and I. Walker, Task-based tracking control of redundant robot manipulators via quaternion feedback, IEEE Transactions on Robotics and Automation, vol. 20, no. 1, pp. 160-167, 2004.

[37] P.B. Petrovic and N.A. Lukic, Configuration-based compliance control of kinematically redundannt robot arm, Part I: Theoretical Framework, Transactions of the Faculty of Mechanical Engineering, Univ, of Belgrade, Feb. 2017.

[38] G. Chiaverini, G. Oriolo and A.a. Maciejewski, Redundant robots, Springer Handbooks on Robotics, 2nd Edition, pp. 221-242, 2016.

[39] A. Karami, H. Sadeghian, M. Keshmiri and G. Oriolo, Force orientation and position control in redundant manipulators in prioritized scheme with null space compliance, Control Engineering Practice, Elsevier, vol. 85, pp. 23-33, 2019.

[40] J. Woolfrey, W. Lu and D. Liu, A control method for joint-torque minimization of redundant manipulators handling large external forces, Journal of Intelligent and Robotic Systems, Springer, vol. 93, pp. 3-16, 2019.

[41] C. Shen, Y. Shi, and B. Buckham, Path-Following Control of an AUV: A Multiobjective Model Predictive Control Approach, IEEE Transactions on Control Systems Technology, vol. 27, no. 3, pp. 1334-1343, 2019.

[42] C. Shen, Y. Shi and B. Buckham, Trajectory tracking control of an autonomous underwater vehicle using Lyapunov-based Model Predictive Control, IEEE Transactions on Industrial Electronids, vol. 65, no. 7, pp. 5796-5805, 2018.

[43] C. Shen, B. Buckham abd Y. Shi, Modified C/GMRES algorithm for fast Nonlinear Model Predictive Tracking Control of AUVs, IEEE Transactions on Control Systems Technology, vol. 25, no. 5, pp. 1896-1905, 2017.

[44] H. Choukri Lamraoui and Z. Qidan, Path following control of fully actuated autonomous underwater vehicle in presence of fast varying disturbances, Applied Ocean Research, Elsevier, vol. 88, pp. 40-46, 2019.

[45] J. Guerrero, J. Torres, V. Creuze and A. Chemori, Observation-based nonlinear Proportial Derivative control for robust trajectory tracking for Autonomous Underwater Vehicles, IEEE Journal of Oceanic Engineering, 2019

[46] C. Zacarrias Ferreira, R. Cardoso, M.E. Mendosa Mesa and J.P. Julca Avila, Controlling tracking trajectory of a robotic vehicle for inspection of underwater structures, Ocean Engineering, Elsevier, vol. 149, pp. 373-382, 2-018.

[47] C.D. Makavita, S.G. Jayasingh, H.D. Mguyen and D. Ranmurthugala, Experimental study of command governor adaptive control for unmanned underwater vehicles, IEEE Transactions on Control Systems Technology, vol. 27, no. 1, pp. 332-345, 2019.

[48] X. Ying, J. Yan, C. Hun and X. Guan, Trajectory tracking control of autonomous underwater vehicle with unknown parameter and external disturbances, IEEE Transactions on Systems, Man and Cybernetics: Systems, 2020.

[49] Z. Yan, Z. Yang, I. Zhang, J. Zhou, A. Jiang an X. Du, Trajectory tracking control of UUV based on backstepping sliding-mode with fuzzy switching gain in diving plane, IEEE Access, vol. 7, pp. 166788-166795, 2019.

[50] G. Allibert, M.D. Hua, S. Krupinsky and T. Hamel, Pipeline following by visual servoing for autonomous underwater vehicles, Control Engineering Practive, Elsevier, vol 82, pp. 151-160, 2019.

[51] R.A. Suarez Fernandez, D. Grande, A. Martins, L. Bascetta, S. Dominguez and C. Rossi, Modelling and control of underwater mine explorer robot UX-1, IEEE Access, vol. 7, pp. 39452-39465, 2019.

[52] X. Xiang, L. Lapierre and B. Jouvencel, Smooth transition of AUV motion control: From fully actuated to under-actuated configuration, Robotics and Autonomous Systems, Elsevier, vol, 67, pp. 14-22, 2015.

[53] N. Fischer, D. Hughes, P. Walters, E.M. Schwartz and W.E. Dixon, Nonlinear RISE-based control of an autonomous underwater vehicle, IEEE Transactions on Robotics, vol. 30, no. 4, pp. 845-853, 2014.

[54] X. Xiang, G. Yu and Q. Zhang, Robust fuzzy 3D path following for autoonomous underwater vehicle subject to uncertainties , Computers and Operations Research, Elsevier, vol. 84, pp. 165-177, 2017.

[55] L. Qiao and W. Zhang, Adaptive non-singular integral terminal slding-mode tracking control for autonomous underwater vehicles, IET Control Theory and Applications, vol. 11, no. 8, pp. 1293-1306, 2017.

[56] Z. Ma, J. Hu, J. Feng and A. Liu, Diving adaptive position tracking control for underactuated vehicles, IEEE Access, vol. 7, pp. 24602-24611, 2019.

[57] Z. Peng, J. Wang and J. Wang, Constrained control of autonomous underwater vehicles based on command optimization and disturbance estimation, IEEE Transactions on Industrial Electronics, vol. 66, no. 5, pp. 3627-3635, 2019.

[58] C. Yu, X. Xiang, P.A. Wilson and Q. Zhang, Guidance-error-based robot adaptive control for bottom following of a flight-style AUV with saturated actuator dynamics, IEEE Transactions on Cybernetics, 2020.

[59] R. Xu, D. Tang, L. Hun, H. Huang and D. Xie. Robust finite-time attitude tracking control of aCMG-based AUV with unknown disturbances and inpur saturation, IEEE Access, vol. 7, pp. 56409-56423, 2019.

[60] Y. Zhang, X. Liu, M. Luo and C. Yang, MPC-based 3D trajectory tracking for an autonomous underwater vehicle with constraints in complex ocean environments, Ocean Engineering, vol. 189, pp. 106309, 2019.

[61] B. Narayan Rath abd D. Subudhi, Online extreme learning algorithm based identification and Nonlinear Model Predictive Controller for way-point tracking application of an autonomous underwater vehicle, IET Cognitive Computation and Systems, vol. 1, no. 3, pp. 61-71, 2019.

[62] H. Wei, C. Shen and Y. Shi, Distributed Lyapunov-based Model Predictive Formation Tracking Control for Autonomous Underwater Vehicles subject to disturbances, IEEE Transactions on Systems, Man and Cybernetics, 2020.

[63] J. Guo, G. Zhang, P. Wu, Z. Zhao, T. Wang and W. Yan, Model Predictive Visual Servoing of fully-actuated underwater vehicles with a sliding-mode disturbance observer, IEEE Access, vol. 7, pp. 25516-25527, 2019.

**Appendix: Comparison between flatness-based control in successive loops and backstepping control**

Backstepping control can be applied to nonlinear dynamical systems in the triangular form. A backstepping control law can be derived for systems of the form [1],[16]:

$$\begin{matrix} \dot{x} = f(x) + g(x)u \\ y = h(x) \end{matrix} \tag{62}$$

for which holds

$$\dot{y} = \frac{\partial h(x)}{\partial x}\dot{x} = \frac{\partial h(x)}{\partial x}[f(x) + g(x)u] = L_f h(x) + L_g h(x)u \tag{63}$$

where the Lie derivatives are defined as

$$L_f h(x) = \frac{\partial}{\partial x}h(x)f(x), \;\; L_g h(x) = \frac{\partial}{\partial x}h(x)g(x) \tag{64}$$

The system of Eq. (62) can be written in cascading form

$$\begin{matrix} \dot{x}_1 = f_1(x_1) + g_1(x_1)x_2 \\ \dot{x}_2 = f_2(x_1, x_2) + g_2(x_1, x_2)x_3 \\ \dot{x}_3 = f_3(x_1, x_2, x_3) + g_3(x_1, x_2, x_3)x_4 \\ \cdots \;\; \cdots \\ \cdots \;\; \cdots \\ \dot{x_{n_1}} = f_{n-1}(x_1, x_2, \cdots, x_{n-1}) + g_{n-1}(x_1, x_2, \cdots, x_{n-1})x_n \\ \dot{x_n} = f_n(x_1, x_2, \cdots, x_n) + g_{n-1}(x_1, x_2, \cdots, x_n)u \\ \\ y = h(x_1) \end{matrix} \tag{65}$$

Then, the $n$-th order backstepping SISO controller is given by the recursive relation

$$\begin{matrix} \alpha_1 = \frac{1}{L_{g_1}h(x_1)}[\dot{y}_d - L_{f_1}h(x_1) - k_1 z_1 - n_1(z_1)z_1] \\ \alpha_2 = \frac{1}{L_{g_2}h(x_1,x_2)}[\dot{\alpha}_1 - f_2(x_1, x_2) - L_{g_1}h(x_1)z_1 - k_2 z_2 - n_2(z_2)z_2] \\ \cdots \\ \alpha_i = \frac{1}{L_{g_i}h(x_1,x_2,\cdots,x_i)}[\dot{\alpha}_{i-1} - f_i(x_1, \cdots, x_i) - g_{i-1}(x_1, x_2, \cdots, x_{i-1})z_{i-1} - k_i z_1 - n_i(z_i)z_i] \\ \cdots \\ \alpha_n = \frac{1}{L_{g_n}h(x_1,x_2,\cdots,x_n)}[\dot{\alpha}_{n-1} - f_n(x_1, \cdots, x_n) - g_{n-1}(x_1, x_2, \cdots, x_{n-2})z_{n-1} - k_n z_n - n_n(z_n)z_n] \\ \\ u = \alpha_n \end{matrix} \tag{66}$$

with $z_1 = h(x_1) - y_d$ and $z_i = x_i - \alpha_{i-1}$. Such a backstepping controller results in closed-loop dynamics given by $\dot{z} = -K(z)z + S(x)z$, with

$$K(z) = \begin{pmatrix} k_1 + n_1(z_1) & 0 & \cdots & 0 \\ 0 & k_2 + n_2(z_2) & \cdots & 0 \\ \cdots & \cdots & \cdots & \cdots \\ 0 & 0 & \cdots & k_n + n_n(z_n) \end{pmatrix} \tag{67}$$

$$
S(x)=\begin{pmatrix}
0 & L_{g_1}(x_1) & 0 & \cdots & 0 & 0 & 0 \\
-L_{g_1}(x_1) & 0 & g_2(x_1,x_2) & 0 & 0 & 0 & \\
0 & -g_2(x_1,x_2) & 0 & \cdots & 0 & 0 & 0 \\
\cdots & \cdots & \cdots & \cdots & \cdots & \cdots & \cdots \\
0 & 0 & 0 & \cdots & 0 & g_{n-1}(x_1,\cdots,x_{n-1}) & 0 \\
0 & 0 & 0 & \cdots & -g_{n-1}(x_1,\cdots,x_{n-1}) & 0 & 0 \\
0 & 0 & 0 & \cdots & 0 & -g_n(x_1,\cdots,x_n & 0)
\end{pmatrix} \tag{68}
$$

From the above it can be noticed that the so-called backstepping control, which is based on the recursive computation of the control signal of the system after applying virtual control inputs to the individual rows of the state-space model, can be completely substituted by the proposed flatness-based control method. A backstepping control law can be derived for systems of the triangular form [1],[16]. However, as it was previously analyzed, by showing that each row of the state-space model stands for a subsystem that satisfies differential flatness properties one can apply effectively to each subsystem the controller design stages found in input-output linearizing flatness-based control methods.

**Funding Statement**: The research work entitled "Flatness-based control in successive loops for robotic manipulators and autonomous vehicles" has been partially supported by Grant Ref. "CSP_contract_040322" - "Nonlinear control, estimation and fault diagnosis for electric power generation and electric traction / propulsion systems" of the Unit of Industrial Automation of the Industrial Systems Institute.

**Authors' contribution statement**: The authors state that their contribution to the research work entitled "Flatness-based control in successive loops for robotic manipulators and autonomous vehicles" is in accordance to their order of appearance of their names in the article's list of authors.

**Competing interests statement**: The authors state that to their knowledge no conflict exists with other members of the scientific community or third parties about the contents of the article "Flatness-based control in successive loops for robotic manipulators and autonomous vehicles".